Acta Cryst E CRYSTALLOGRAPHIC COMMUNICATIONS
ISSN 2056-9890

2-[(2,4,6-Trimethylbenzene)sulfonyl]phthalazin-1(2*H*)-one: crystal structure, Hirshfeld surface analysis and computational study

David Chukwuma Izuogu,[a,b,c] Jonnie Niyi Asegbeloyin,[a]‡ Mukesh M. Jotani[d] and Edward R. T. Tiekink[e]*

[a]Department of Pure and Industrial Chemistry, University of Nigeria, Nsukka 410001, Enugu State, Nigeria, [b]Department of Chemistry, Graduate School of Science, Tohoku University, 6-3 Aza-aoba, Aramaki, Sendai 980-8578, Japan, [c]Department of Chemistry, University of Cambridge, Lensfield Road, CB2 1EW, UK, [d]Department of Physics, Bhavan's Sheth R. A. College of Science, Ahmedabad, Gujarat 380001, India, and [e]Research Centre for Crystalline Materials, School of Science and Technology, Sunway University, 47500 Bandar Sunway, Selangor Darul Ehsan, Malaysia. *Correspondence e-mail: edwardt@sunway.edu.my

Received 6 April 2020
Accepted 11 April 2020

Edited by A. J. Lough, University of Toronto, Canada

‡ Additional correspondence author, e-mail: niyi.asegbeloyin@unn.edu.ng.

Keywords: crystal structure; phthalazinone; Hirshfeld surface analysis.

CCDC reference: 1996401

Supporting information: this article has supporting information at journals.iucr.org/e

The X-ray crystal structure of the title phthalazin-1-one derivative, $C_{17}H_{16}N_2O_3S$ {systematic name: 2-[(2,4,6-trimethylbenzene)sulfonyl]-1,2-dihydrophthalazin-1-one}, features a tetrahedral sulfoxide-S atom, connected to phthalazin-1-one and mesityl residues. The dihedral angle [83.26 (4)°] between the organic substituents is consistent with the molecule having the shape of the letter *V*. In the crystal, phthalazinone-C_6-C—H···O(sulfoxide) and π(phthalazinone-N_2C_4)–π(phthalazinone-C_6) stacking [inter-centroid distance = 3.5474 (9) Å] contacts lead to a linear supramolecular tape along the *a*-axis direction; tapes assemble without directional interactions between them. The analysis of the calculated Hirshfeld surfaces confirm the importance of the C—H···O and π-stacking interactions but, also H···H and C—H···C contacts. The calculation of the interaction energies indicate the importance of dispersion terms with the greatest energies calculated for the C—H···O and π-stacking interactions.

1. Chemical context

Phthalazin-1(2*H*)-one derivatives are a group of diaza-heterobicycles that are noteworthy for their interesting medicinal applications. Thus, this class of compound has been reported to possess a wide variety of biological properties such as anti-diabetic (Mylari *et al.*, 1992), anti-cancer (Menear *et al.*, 2008), anti-inflammatory and analgesic (Pakulska *et al.*, 2009), anti-histamine (Procopiou *et al.*, 2011), anti-hypertensive and anti-thrombotic (Cherkez *et al.*, 1986) activities. Some N-substituted phthalazinones have attracted attention as a result of their potential role as anti-asthmatic agents (Ukita *et al.*, 1999), their ability to inhibit thromboxane A2 (TXA2) synthetase and to induce bronchodialation (Yamaguchi *et al.*, 1993). At the present time, a number of phthalazin-1(2*H*)-one-based drugs are in use (Wu *et al.*, 2012; Teran *et al.*, 2019). A number of reaction pathways to the phthalazinone skeleton are known, notable among which include multi-step reactions involving cyclocondensation reactions of phthalic anhydrides, phthalimides, phthalaldehydic acid or 2-acylbenzoic acids with substituted hydrazines, in the presence of appropriate catalysts (Haider & Holzer, 2004). The conversion of phthalimides *via* Friedel–Crafts conditions or with organometallics to 2-keto benzoic acid hydrazides or 3,3-disubstituted indolinones, which are viable intermediates to substituted phthalazin-

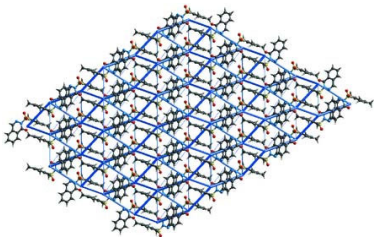

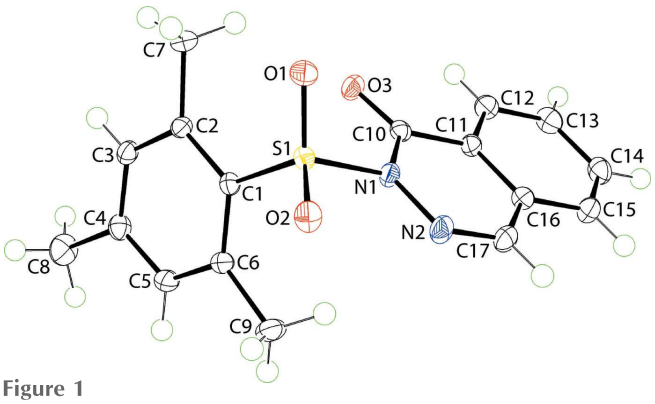

Figure 1
The molecular structures of (I) showing the atom-labelling scheme and displacement ellipsoids at the 70% probability level.

1(2*H*)-ones, have also been reported (Ismail *et al.*, 1984; Chun *et al.*, 2004) . Several other synthetic routes, involving various intermediates, have also been reported (Mylari *et al.*, 1991; Yamaguchi *et al.*, 1993; Acosta *et al.*, 1995; Bele & Darabantu, 2003; Mahmoodi & Salehpour, 2003; Cockcroft *et al.*, 2006; Del Olmo *et al.*, 2006). In an earlier communication (Asegbeloyin *et al.*, 2018), the dysprosium(III)-catalysed conversion of 2-{[2-(phenylsulfonyl)hydrazinylidene] methyl}benzoic acid to 2-(phenylsulfonyl)phthalazin-1-(2*H*)-one was described. In the present study, the title compound, 2-[(2,4,6-trimethylbenzene)sulfonyl]-1,2-dihydrophthalazin-1-one, (I), was obtained by the catalytic conversion of 2-{[2-(2,4,6-trimethylphenylsulfonyl)hydrazinylidene]methyl}benzoic acid. Herein, the crystal and molecular structures of (I) are described as is a detailed analysis of the molecular packing by an evaluation of the calculated Hirshfeld surfaces augmented by a computational chemistry study.

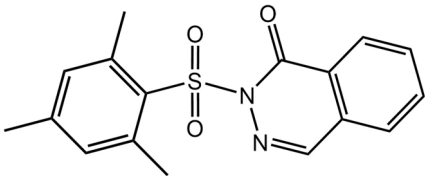

Table 1
Hydrogen-bond geometry (Å, °).

D—H···*A*	*D*—H	H···*A*	*D*···*A*	*D*—H···*A*
C12—H12···O2^{i}	0.95	2.49	3.3395 (18)	149

Symmetry code: (i) $x, y-1, z$.

2. Structural commentary

The molecule of (I), Fig. 1, may be conveniently described as a central SO_2 residue with mesityl and phthalazin-1-one substituents. The geometry about the S1 atom is distorted tetrahedral with the range of angles subtended at S1 being a narrow 103.58 (6)° for N1—S1—C1, involving the singly-bonded N1 and C1 atoms, to a wide 118.39 (6)°, for O1—S1—O2, involving the doubly-bonded sulfoxide-O1, O2 atoms. The organic residues lie to the opposite side of the molecule to the SO_2 residue, forming dihedral angles of 67.35 (4)° [phthalazin-1-one with r.m.s. deviation = 0.0105 Å] and 49.79 (6)° [mesityl]. The dihedral angle between the organic residues of 83.26 (4)° indicates a close to orthogonal relationship. The N2—N1—C10—O3 torsion angle of −179.88 (12)° indicates a co-planar arrangement for these atoms, which allows for the close approach of the N2 and O3 atoms, *i.e.* 2.6631 (15) Å, suggestive of a stabilizing contact (Nakanishi *et al.*, 2007). Globally, the molecule has the shape of the letter *V*. Within the hetero-ring of the phthalazin-1-one substituent, the N1—N2 bond length is 1.3808 (15) Å and C10—N1 = 1.4003 (17) Å. In each of the C17═N2 [1.2911 (18) Å] and C10═O3 [1.2175 (15) Å] bonds, double-bond character is noted. The bond angles about the N1 atom are non-symmetric, with the endocyclic N2—N1—C10 angle of 126.97 (11) Å being significantly wider than the exocyclic N2—N1—S1 [113.93 (9) Å] and C10—N1—S1 [118.89 (8) Å] angles.

3. Supramolecular features

The formation of a supramolecular tape sustained by phthalazinone-C_6-C—H···O(sulfoxide) contacts, Table 1, and π(phthalazinone)–π(phthalazinone) stacking is the main feature of the molecular packing in the crystal of (I), Fig. 2(*a*).

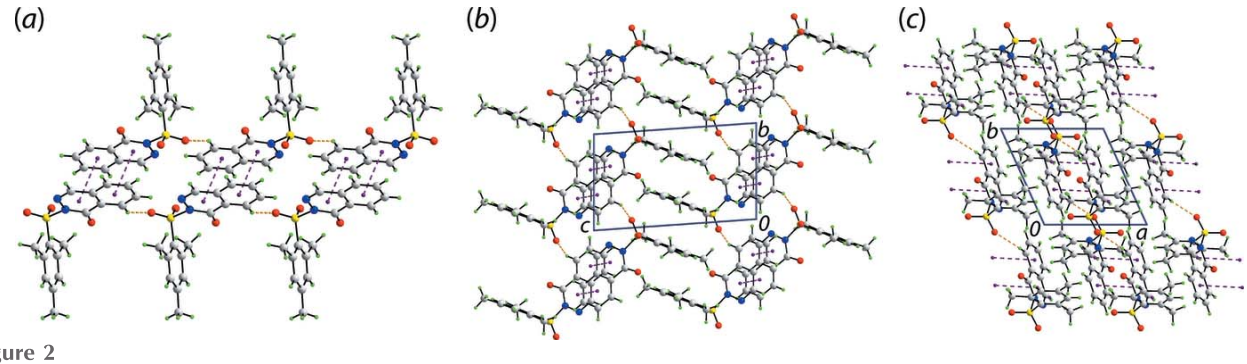

Figure 2
Molecular packing in the crystal of (I): (*a*) supramolecular tape sustained by phthalazinone-C—H···O(sulfoxide) and π(phthalazinone)–π(phthalazinone) stacking interactions shown as orange and purple dashed lines, respectively, (*b*) a view of the unit-cell contents down the *a* axis showing the inter-digitation of tapes and (*c*) a view of the unit-cell contents down the *c* axis showing the stacking of assemblies of (*b*) along the *a*-axis direction.

Table 2
A summary of short interatomic contacts (Å) in (I)[a].

Contact	Distance	Symmetry operation
C10···C14	3.345 (2)	$1-x, 1-y, 2-z$
C12···C16	3.351 (2)	$1-x, 1-y, 2-z$
O1···H9*C*	2.58	$1+x, y, z$
O1···H14	2.61	$1-x, 1-y, 2-z$
O3···H8*A*	2.60	$-x, 1-y, 1-z$
C5···H7*C*	2.78	$1-x, 2-y, 1-z$
C7···H5	2.61	$1+x, y, z$
C10···H8*A*	2.79	$-x, 1-y, 1-z$
H12···H9*A*	2.20	$x, -1+y, z$

Notes: (*a*) The interatomic distances are calculated in *Crystal Explorer 17* (Turner *et al.*, 2017) whereby the *X*—H bond lengths are adjusted to their neutron values; (*b*) these interactions correspond to conventional hydrogen bonds.

The π-stacking occurs between centrosymmetrically related phthalazinone rings, *i.e.* between the N_2C_4 and C_6^{i} rings with an inter-centroid distance = 3.5474 (9) Å, angle of inclination = 1.17 (7)° for symmetry operation (i) $1-x, 1-y, 2-z$. As shown in Fig. 2(*b*), the tapes inter-digitate along the *c*-axis direction allowing for putative π-stacking between mesityl rings but, the inter-centroid separation is long at 4.1963 (8) Å. The assemblies shown in Fig. 2(*b*) stack along the *a*-axis direction, again without directional interactions between them, Fig. 2(*c*).

4. Hirshfeld surface analysis

In order to probe the interactions between molecules of (I) in the crystal, the Hirshfeld surfaces and two-dimensional fingerprint plots were calculated with the program *Crystal Explorer 17* (Turner *et al.*, 2017) using established procedures described by Tan *et al.* (2019). In addition to the bright-red spots appearing near the sulfoxide-O2 and phthalazinone-H12 atoms on the Hirshfeld surface in Fig. 3(*a*),(*b*), the presence of diminutive red spots near methyl-C7 and benzene-H5 are indicative of intermolecular C—H···C contacts as C—H···π contacts are not preferred because of the *V*-shaped molecular geometry of (I). Also, the group of faint-red spots near alternate carbon atoms C10, C12, C14 and C16 of the phthalazinone-C_6 ring on the d_{norm}-mapped Hirshfeld surface in Fig. 3(*b*) is indicative of short intra-chain C···C contacts

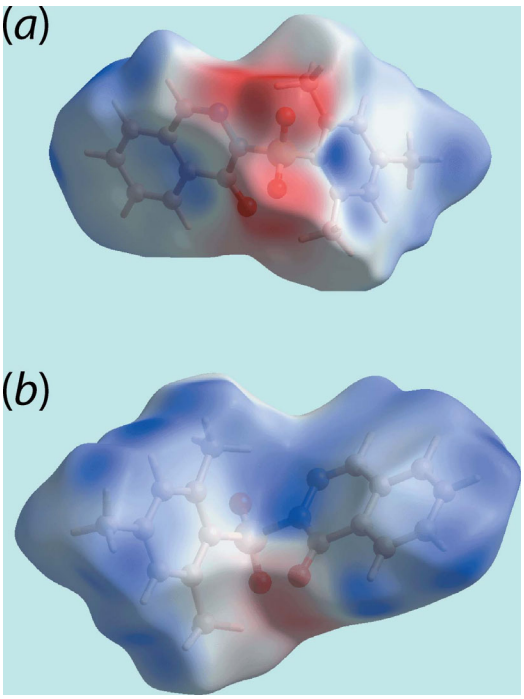

Figure 4
(*a*) and (*b*) Two views of the calculated electrostatic potential mapped onto the Hirshfeld surface within the isosurface range −0.093 to 0.040 atomic units. The red and blue regions represent negative and positive electrostatic potentials, respectively.

[Table 2 and Fig. 2(*a*)] and is consistent with the significant contribution from π–π stacking between centrosymmetrically related phthalazinone-N_2C_4 and C_6 rings, encompassing connections between phthalazinone-C_6 rings [3.6657 (9) Å with angle of inclination = 0.03 (7)°]. The involvement of the methyl-C8 atom in C—H···O [to provide links between the chains shown in Fig. 2(*b*)] and C—H···C contacts, Table 2, is highlighted in Fig. 3(*c*). The blue and red regions corresponding to positive and negative electrostatic potentials, respectively, on the Hirshfeld surface mapped over electrostatic potential shown in Fig. 4 represent the involvement of different atoms in the intermolecular interactions in the crystal.

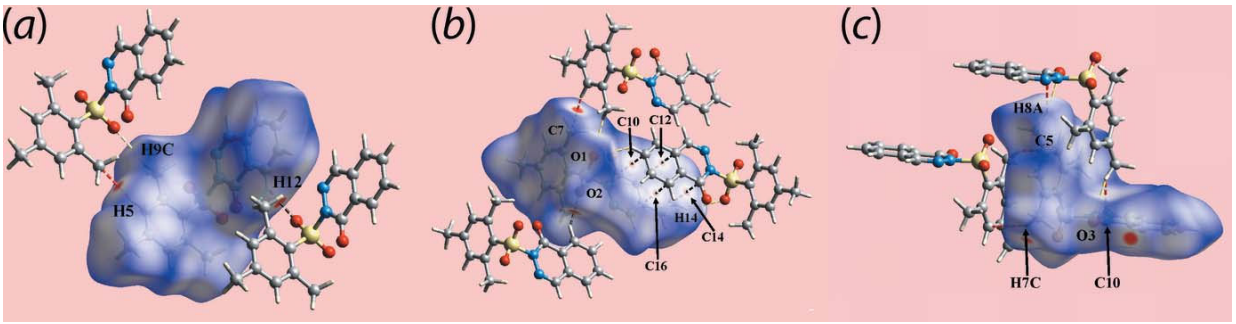

Figure 3
(*a*)–(*c*) Three views of Hirshfeld surface mapped over d_{norm} for (I) in the range −0.128 to + 1.298 arbitrary units. The intermolecular C-H···O and short interatomic C···C contacts are represented with black dashed lines, and the short interatomic H···H, O···H/H···O and C···H/H···C contacts with sky-blue, yellow and red dashed lines, respectively.

Table 3
Percentage contributions to intermolecular contacts on the Hirshfeld surface calculated for (I).

Contact	Percentage contribution
H···H	44.9
O···H/H···O	24.0
C···H/H···C	18.1
C···C	6.5
N···H/H··· N	4.0
C···O/O···C	1.1
C···N/N···C	0.7
N···N	0.4
C···S/S···C	0.2

The overall two-dimensional fingerprint plots for (I) and those delineated into H···H, O···H/H···O, C···H/H···C and C···C contacts are illustrated in Fig. 5(*a*)–(*e*), respectively; the percentage contributions from the different interatomic contacts to the Hirshfeld surfaces are summarized in Table 3. A short interatomic H···H contact involving the phthalazinone-H12 and methyl-H9*A* atoms, Table 2, appears as a small peak at $d_e + d_i$ ~2.2 Å in the fingerprint plot delineated into H···H contacts, Fig. 5(*b*). In the fingerprint plot delineated into O···H/H···O contacts illustrated in Fig. 5(*c*), a pair of forceps-like tips at $d_e + d_i$ ~2.3 Å, indicate the intermolecular C—H···O interaction involving the phthalazinone-H12 and sulfoxide-O2 atoms, whereas the other interatomic O···H/H···O contacts are merged within the plot and appear as a pair of intense blue spikes at $d_e + d_i$ ~2.8 Å. Despite the observation that intermolecular C—H···π contacts are usually preferred by methyl groups, none are found involving those substituted at (C1–C6) benzene ring in the crystal due to the *V*-shaped geometry. Rather, the involvement of methyl-C7 and H5*A* atoms, and benzene-C5 and H7*C* atoms [to provide links between the chains shown in Fig. 2(*b*)] in C—H···C interactions, Table 2, are characterized as the pair of forceps-like flat tips about $d_e + d_i$ ~2.8 Å in the fingerprint plot delineated into C···H/H···C contacts, Fig. 5(*d*). The presence of π–π stacking interactions between symmetry-related phthalazinone-N_2C_4 and C_6 rings is also evident as the arrow-shaped distribution of points around d_e, d_i ~1.8 Å in the fingerprint plot delineated into C···C contacts, Fig. 5(*e*). The contribution from other interatomic contacts, summarized in Table 2, show a negligible effect on the calculated Hirshfeld surface of (I).

Table 4
A summary of interaction energies (kJ mol^{-1}) calculated for (I).

Contact	R (Å)	E_{ele}	E_{pol}	E_{dis}	E_{rep}	E_{tot}
$Cg(N_2C_4)\cdots Cg(C_6)^{i}$ + $Cg(C_6)\cdots Cg(C_6)^{i}$ + O1···H14^{i}	8.12	−28.9	−5.0	−64.7	48.2	−60.8
C5···H7C^{ii}	7.84	−21.3	−5.5	−60.9	43.5	−52.8
O3 ···H8A^{iii} + C10 ···H8A^{iii}	7.54	−10.7	−2.0	−56.8	32.6	−42.1
C12—H12···O2^{iv} + H12···H9A^{iv}	8.17	−4.4	−4.6	−20.5	18.0	−14.8
O1···H9C^{v} + C7···H5^{v}	7.98	−3.1	−2.0	−16.9	14.2	−10.6

Symmetry codes: (i) $1-x, 1-y, 2-z$; (ii) $1-x, 2-y, 1-z$; (iii) $-x, 1-y, 1-z$; (iv) $x, -1+y, z$; (v) $1+x, y, z$.

5. Computational chemistry

The pairwise interaction energies between the molecules within the crystal of (I) were calculated by summing up four energy components, comprising electrostatic (E_{ele}), polarization (E_{pol}), dispersion (E_{dis}) and exchange–repulsion (E_{rep}) following Turner *et al.* (2017). The energies were obtained by using the wave function calculated at the B3LYP/6-31G(*d*,*p*) level of theory. The nature and strength of the intermolecular interactions in terms of their energies are quantitatively summarized in Table 4, where it is clear that the dispersive component makes the major contribution to the interaction energies in the crystal in the absence of conventional hydrogen bonding. It is revealed from the interaction energies listed in Table 4, that the π–π stacking interaction between phthalazinone-N_2C_4 and C_6 rings and the short interatomic O1···H14 contact have the greatest energy. The short interatomic C5···H7*C*, O3···H8*A* and C10···H8*A* contacts also have significant interaction energies due to their participation in inversion-related contacts. Lower energies, compared to above interactions, are calculated for the H12···H9*A*, C7···H5 and O1···H9*C* contacts.

Fig. 6 illustrates the magnitudes of intermolecular energies represented graphically by energy frameworks to highlight the supramolecular architecture of the crystal through cylinders joining the centroids of molecular pairs using red, green and blue colour codes for the components E_{ele}, E_{disp} and E_{tot}, respectively. The images emphasize the importance of dispersion interactions in the molecular packing.

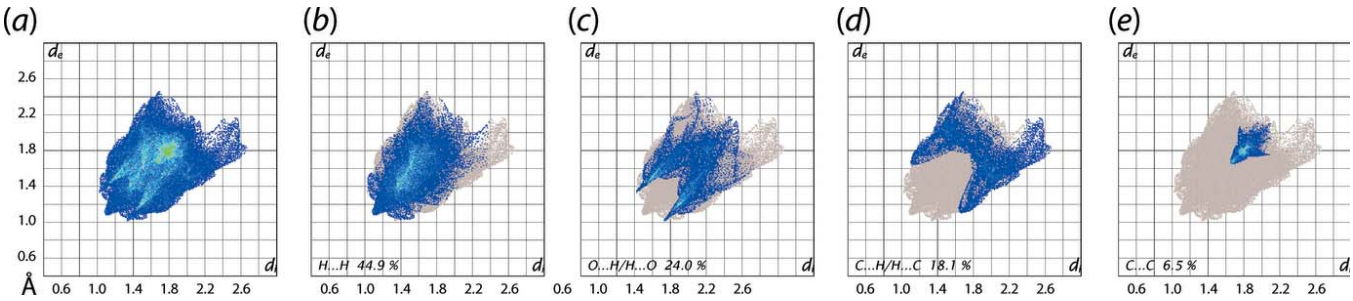

Figure 5
(*a*) The overall two-dimensional fingerprint plots for (I), and those delineated into (*b*) H···H, (*c*) O···H/H···O, (*d*) C···H/H···C and (*e*) C···C contacts.

Table 5
A comparison of key geometric parameters (Å, °) for (I) and (II).

	(I)	(II)
N1—N2	1.3808 (15)	1.384 (2)
C10—O3	1.2175 (15	1.212 (3)
C10—N1	1.4003 (17)	1.406 (2)
C17—N2	1.2911 (18)	1.283 (2)
N2···O2	2.6631 (15)	2.6394 (19)
N2—N1—S1—O1	120.33 (10)	138.71 (12)
N2—N1—S1—O2	−5.52 (11)	9.59 (13)
N1—S1—C1—C2	−111.55 (11)	−103.95 (16)
N1—S1—C1—C6	69.70 (11)	76.49 (17)

6. Database survey

There is only a single direct analogue to (I) in the crystallographic literature, namely 2-(phenylsulfonyl)phthalazin-1(2*H*)-one (Asegbeloyin *et al.*, 2018), (II). A comparison of key geometric parameters for (I) and (II) is given in Table 5. The data in Table 5 confirm the closeness of the salient bond lengths, but also show significant differences in the torsion angles about the N1—S1 and C1—S1 bonds, *i.e.* by up to 18 and 8°, respectively. These conformational differences are highlighted in the overlay diagram of Fig. 7 and in the dihedral angles between the aromatic residues of 83.26 (4) and 78.12 (4)° for (I) and (II), respectively.

7. Synthesis and crystallization

2-{[2-(2,4,6-Trimethylphenylsulfonyl)hydrazinylidene]methyl}benzoic acid (III) was obtained by a method reported earlier (Asegbeloyin *et al.*, 2018). Compound (I) was obtained from the following reaction. An ethanol solution (10 ml) of $Dy(O_2CCH_3)_3{\cdot}4H_2O$ (Wako Chemicals, Japan; 1 mmol, 411.692 mg) was added with constant stirring to an ethanol solution (20 ml) of (III) (1,039.2 mg, 3 mmol). The resulting mixture was refluxed for 3 h in an oil bath. The obtained colourless solution was concentrated to afford a colourless precipitate, which was filtered, dried under suction and further dried *in vacuo* over $CaCl_2$. The precipitates were dissolved in ethanol, the resultant colourless solution was filtered and left at room temperature for 48 h to obtain colourless crystals of (I).

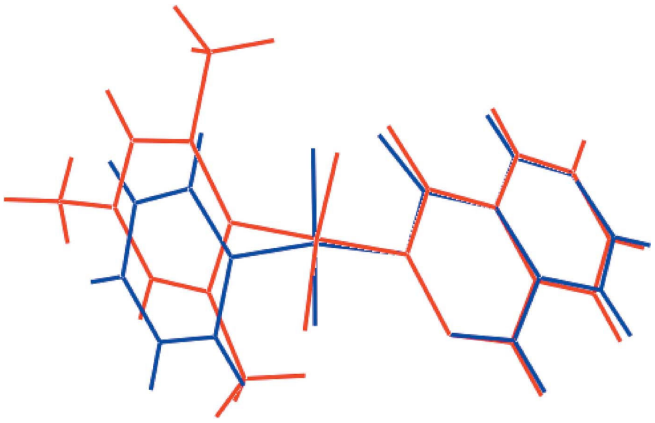

Figure 7
An overlay diagram for (I) (red image) and (II) (blue). The molecules have been overlapped so the hetero-rings are coincident.

8. Refinement

Crystal data, data collection and structure refinement details are summarized in Table 6. The carbon-bound H atoms were placed in calculated positions (C—H = 0.95–0.98 Å) and were included in the refinement in the riding-model approximation, with U_{iso}(H) set to 1.2–1.5U_{eq}(C).

Acknowledgements

The authors are grateful to Professor Masahiro Yamashita of the Department of Chemistry, Tohoku University, for the X-ray intensity data.

Funding information

Crystallographic research at Sunway University is supported by Sunway University Sdn Bhd (grant No. STR-RCTR-RCCM-001-2019).

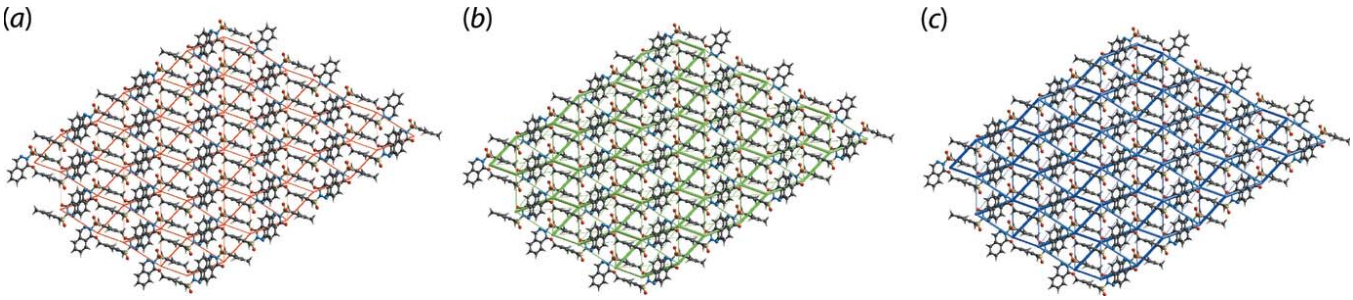

Figure 6
Perspective views of the energy frameworks calculated for (I), showing the (*a*) electrostatic force, (*b*) dispersion force and (*c*) total energy. The radii of the cylinders are proportional to the relative strength of the corresponding energies and were adjusted to the same scale factor of 50 with a cut-off value of 3 kJ mol^{-1} within 4 × 4 × 4 unit cells.

Table 6
Experimental details.

Crystal data	
Chemical formula	$C_{17}H_{16}N_2O_3S$
M_r	328.38
Crystal system, space group	Triclinic, $P\overline{1}$
Temperature (K)	100
a, b, c (Å)	7.9782 (4), 8.1711 (5), 12.6661 (7)
α, β, γ (°)	92.214 (2), 93.423 (1), 114.274 (1)
V (Å^3)	749.55 (7)
Z	2
Radiation type	Mo $K\alpha$
μ (mm^{-1})	0.23
Crystal size (mm)	0.38 × 0.12 × 0.08
Data collection	
Diffractometer	Bruker APEXII CCD
Absorption correction	Multi-scan (*SADABS*; Sheldrick, 1996)
T_{min}, T_{max}	0.924, 1.000
No. of measured, independent and observed [$I > 2\sigma(I)$] reflections	11665, 5913, 4625
R_{int}	0.027
(sin $\theta/\lambda)_{max}$ (Å^{-1})	0.804
Refinement	
$R[F^2 > 2\sigma(F^2)]$, $wR(F^2)$, S	0.048, 0.122, 1.02
No. of reflections	5913
No. of parameters	211
H-atom treatment	H-atom parameters constrained
$\Delta\rho_{max}$, $\Delta\rho_{min}$ (e Å^{-3})	0.59, −0.39

Computer programs: *APEX2* and *SAINT* (Bruker, 2002), *SHELXT* (Sheldrick, 2015*a*), *SHELXL2018/3* (Sheldrick, 2015*b*), *ORTEP-3 for Windows* (Farrugia, 2012), *DIAMOND* (Brandenburg, 2006) and *publCIF* (Westrip, 2010).

References

Acosta, A., de la Cruz, P., De Miguel, P., Diez-Barra, E., de la Hoz, A., Langa, F., Loupy, A., Majdoub, M., Martin, N., Sanchez, C. & Seoane, C. (1995). *Tetrahedron Lett.* **36**, 2165–2168.

Asegbeloyin, J. N., Izuogu, D. C., Oyeka, E. E., Okpareke, O. C. & Ibezim, A. (2018). *J. Mol. Struct.* **1175**, 219–229.

Bele, C. & Darabantu, M. (2003). *Heterocycl. Commun.* **9**, 641–646.

Brandenburg, K. (2006). *DIAMOND*. Crystal Impact GbR, Bonn, Germany.

Bruker (2002). *APEX2* and *SAINT*. Bruker AXS Inc., Madison, Wisconsin, USA.

Cherkez, S., Herzig, J. & Yellin, H. (1986). *J. Med. Chem.* **29**, 947–959.

Chun, T. G., Kim, K. S., Lee, S., Jeong, T. S., Lee, H. Y., Kim, Y. H. & Lee, W. S. (2004). *Synth. Commun.* **34**, 1301–1308.

Cockcroft, X. L., Dillon, K. J., Dixon, L., Drzewiecki, J., Kerrigan, F., Loh, V. M. Jr, Martin, N. M. B., Meneara, K. A. & Smith, G. C. M. (2006). *Bioorg. Med. Chem. Lett.* **16**, 1040–1044.

Del Olmo, E., Barboza, B., Ybarra, M. I., Lopez-Perez, J. L., Carron, R., Sevilla, M. A., Bosellid, C. & San Feliciano, A. (2006). *Bioorg. Med. Chem. Lett.* **16**, 2786–2790.

Farrugia, L. J. (2012). *J. Appl. Cryst.* **45**, 849–854.

Haider, N. & Holzer, W. (2004). *Science Synth.* **16**, 315–372.

Ismail, M. F., El-Bassiouny, F. A. & Younes, H. A. (1984). *Tetrahedron* **40**, 983–2984.

Mahmoodi, N. O. & Salehpour, M. J. (2003). *Heterocycl. Chem.* **40**, 875–878.

Menear, K. A., Adcock, C., Boulter, R., Cockcroft, X., Copsey, L., Cranston, A., Dillon, K. J., Drzewiecki, J., Garman, S., Gomez, S., Javaid, H., Kerrigan, F., Knights, C., Lau, A., Loh, V. M. Jr, Matthews, I. T. W., Moore, S., O'Connor, M. J., Smith, G. C. M. & Martin, N. M. B. (2008). *J. Med. Chem.* **51**, 6581–6591.

Mylari, B. L., Beyer, T. A., Scott, P. J., Aldinger, C. E., Dee, M. F., Siegel, T. W. & Zembrowski, W. J. (1992). *J. Med. Chem.* **35**, 457–465.

Mylari, B. L., Larson, E. R., Beyer, T. A., Zembrowski, W. J., Aldinger, C. E., Dee, M. F., Siegel, T. W. & Singleton, D. H. (1991). *J. Med. Chem.* **34**, 108–122.

Nakanishi, W., Nakamoto, T., Hayashi, S., Sasamori, T. & Tokitoh, N. (2007). *Chem. Eur. J.* **13**, 255–268.

Pakulska, W., Malinowski, Z., Szczesniak, A. K., Czarnecka, E. & Epsztajn, J. (2009). *Arch. Pharm. Chem. Life Sci.* **342**, 41–47.

Procopiou, P. A., Browning, C., Buckley, J. M., Clark, K. L., Fechner, L., Gore, P. M., Hancock, A. P., Hodgson, S. T., Holmes, D. S., Kranz, M., Looker, B. E., Morriss, K. M. L., Parton, D. L., Russell, L. J., Slack, R. J., Sollis, S. L., Vile, S. & Watts, C. J. (2011). *J. Med. Chem.* **54**, 2183–2195.

Sheldrick, G. M. (1996). *SADABS*. University of Göttingen, Germany.

Sheldrick, G. M. (2015*a*). *Acta Cryst.* A**71**, 3–8.

Sheldrick, G. M. (2015*b*). *Acta Cryst.* C**71**, 3–8.

Tan, S. L., Jotani, M. M. & Tiekink, E. R. T. (2019). *Acta Cryst.* E**75**, 308–318.

Teran, C., Besada, P., Vila, N. & Costa-Lago, M. C. (2019). *Eur. J. Med. Chem.* **161**, 468–478.

Turner, M. J., Mckinnon, J. J., Wolff, S. K., Grimwood, D. J., Spackman, P. R., Jayatilaka, D. & Spackman, M. A. (2017). *Crystal Explorer 17*. The University of Western Australia.

Ukita, T., Sugahara, M., Terakawa, Y., Kuroda, T., Wada, K., Nakata, A., Ohmachi, Y., Kikkawa, H., Ikezawa, K. & Naito, K. (1999). *J. Med. Chem.* **42**, 1088-1099.

Westrip, S. P. (2010). *J. Appl. Cryst.* **43**, 920–925.

Wu, X.-F., Neumann, H., Neumann, S. & Beller, M. (2012). *Chem. Eur. J.* **18**, 8596-8599.

Yamaguchi, M., Kamei, K., Koga, T., Akima, M., Kuroki, T. & Ohi, N. (1993). *J. Med. Chem.* **36**, 4052–4060.

supporting information

Acta Cryst. (2020). E**76**, 697-702 [https://doi.org/10.1107/S2056989020005101]

2-[(2,4,6-Trimethylbenzene)sulfonyl]phthalazin-1(2*H*)-one: crystal structure, Hirshfeld surface analysis and computational study

David Chukwuma Izuogu, Jonnie Niyi Asegbeloyin, Mukesh M. Jotani and Edward R. T. Tiekink

Computing details

Data collection: *APEX2* (Bruker, 2002); cell refinement: *SAINT* (Bruker, 2002); data reduction: *SAINT* (Bruker, 2002); program(s) used to solve structure: *SHELXS* (Sheldrick, 2015*a*); program(s) used to refine structure: *SHELXL2018/3* (Sheldrick, 2015*b*); molecular graphics: *ORTEP-3 for Windows* (Farrugia, 2012), *DIAMOND* (Brandenburg, 2006); software used to prepare material for publication: *publCIF* (Westrip, 2010).

2-[(2,4,6-Trimethylbenzene)sulfonyl]phthalazin-1(2*H*)-one

Crystal data

$C_{17}H_{16}N_2O_3S$
M_r = 328.38
Triclinic, $P\overline{1}$
a = 7.9782 (4) Å
b = 8.1711 (5) Å
c = 12.6661 (7) Å
α = 92.214 (2)°
β = 93.423 (1)°
γ = 114.274 (1)°
V = 749.55 (7) Å^3
Z = 2
$F(000)$ = 344
D_x = 1.455 Mg m^{-3}
Mo $K\alpha$ radiation, λ = 0.71073 Å
Cell parameters from 5241 reflections
θ = 2.7–34.7°
μ = 0.23 mm^{-1}
T = 100 K
Prism, colourless
0.38 × 0.12 × 0.08 mm

Data collection

Bruker APEXII CCD diffractometer
Radiation source: fine-focus sealed tube
ω scans
Absorption correction: multi-scan (SADABS; Sheldrick, 1996)
T_{min} = 0.924, T_{max} = 1.000
11665 measured reflections
5913 independent reflections
4625 reflections with $I > 2\sigma(I)$
R_{int} = 0.027
θ_{max} = 34.9°, θ_{min} = 1.6°
h = −12→12
k = −13→7
l = −19→19

Refinement

Refinement on F^2
Least-squares matrix: full
$R[F^2 > 2\sigma(F^2)]$ = 0.048
$wR(F^2)$ = 0.122
S = 1.02
5913 reflections
211 parameters
0 restraints
Primary atom site location: structure-invariant direct methods
Secondary atom site location: difference Fourier map
Hydrogen site location: inferred from neighbouring sites
H-atom parameters constrained

$w = 1/[\sigma^2(F_o^2) + (0.0579P)^2 + 0.3671P]$
where $P = (F_o^2 + 2F_c^2)/3$
$(\Delta/\sigma)_{max} < 0.001$

$\Delta\rho_{max} = 0.59$ e Å^{-3}
$\Delta\rho_{min} = -0.39$ e Å^{-3}

Special details

Geometry. All esds (except the esd in the dihedral angle between two l.s. planes) are estimated using the full covariance matrix. The cell esds are taken into account individually in the estimation of esds in distances, angles and torsion angles; correlations between esds in cell parameters are only used when they are defined by crystal symmetry. An approximate (isotropic) treatment of cell esds is used for estimating esds involving l.s. planes.

Fractional atomic coordinates and isotropic or equivalent isotropic displacement parameters (Å^2)

	x	*y*	*z*	U_{iso}*/U_{eq}
S1	0.52952 (4)	0.91549 (4)	0.73039 (2)	0.00972 (8)
O1	0.70758 (13)	0.91524 (14)	0.72487 (8)	0.01414 (19)
O2	0.51875 (14)	1.07825 (13)	0.76724 (7)	0.01422 (19)
O3	0.45530 (14)	0.53580 (14)	0.72961 (7)	0.01357 (19)
N1	0.42015 (15)	0.76225 (15)	0.82277 (8)	0.0107 (2)
N2	0.36966 (17)	0.83676 (16)	0.90820 (9)	0.0138 (2)
C1	0.38648 (17)	0.82486 (17)	0.61201 (9)	0.0097 (2)
C2	0.44783 (17)	0.75451 (17)	0.52613 (10)	0.0103 (2)
C3	0.32852 (18)	0.69064 (18)	0.43396 (10)	0.0116 (2)
H3	0.367189	0.643377	0.375142	0.014*
C4	0.15518 (18)	0.69371 (18)	0.42516 (10)	0.0126 (2)
C5	0.09886 (18)	0.76139 (19)	0.51177 (10)	0.0133 (2)
H5	−0.020289	0.761710	0.506665	0.016*
C6	0.21077 (18)	0.82878 (18)	0.60579 (10)	0.0116 (2)
C7	0.63166 (18)	0.7437 (2)	0.52408 (11)	0.0141 (2)
H7A	0.636640	0.683730	0.456594	0.021*
H7B	0.647194	0.675014	0.582699	0.021*
H7C	0.730720	0.865470	0.531622	0.021*
C8	0.0315 (2)	0.6274 (2)	0.32396 (11)	0.0190 (3)
H8A	−0.094563	0.608096	0.337969	0.028*
H8B	0.032099	0.513741	0.296720	0.028*
H8C	0.076289	0.717057	0.271317	0.028*
C9	0.1341 (2)	0.9043 (2)	0.69211 (11)	0.0190 (3)
H9A	0.184991	1.035634	0.691039	0.028*
H9B	0.168371	0.871735	0.761207	0.028*
H9C	−0.000599	0.854423	0.680026	0.028*
C10	0.40551 (17)	0.58589 (17)	0.80886 (10)	0.0099 (2)
C11	0.32443 (17)	0.47264 (18)	0.89581 (10)	0.0106 (2)
C12	0.30524 (18)	0.29500 (18)	0.89276 (10)	0.0132 (2)
H12	0.343082	0.246095	0.834285	0.016*
C13	0.23047 (19)	0.19062 (19)	0.97587 (11)	0.0153 (3)
H13	0.216814	0.069423	0.974185	0.018*
C14	0.17479 (19)	0.2621 (2)	1.06236 (11)	0.0160 (3)
H14	0.123129	0.189023	1.118763	0.019*
C15	0.19460 (19)	0.4382 (2)	1.06607 (11)	0.0154 (3)
H15	0.157015	0.486375	1.124986	0.018*

C16	0.27053 (18)	0.54625 (18)	0.98247 (10)	0.0118 (2)
C17	0.2996 (2)	0.73194 (19)	0.98264 (10)	0.0145 (2)
H17	0.264466	0.781298	1.042086	0.017*

Atomic displacement parameters (Å²)

	U^{11}	U^{22}	U^{33}	U^{12}	U^{13}	U^{23}
S1	0.00989 (13)	0.01011 (14)	0.00894 (13)	0.00401 (11)	0.00008 (10)	0.00083 (10)
O1	0.0094 (4)	0.0174 (5)	0.0147 (4)	0.0047 (4)	0.0002 (3)	0.0018 (4)
O2	0.0193 (5)	0.0103 (4)	0.0128 (4)	0.0061 (4)	0.0007 (4)	−0.0004 (3)
O3	0.0168 (5)	0.0153 (5)	0.0105 (4)	0.0083 (4)	0.0033 (3)	0.0004 (3)
N1	0.0139 (5)	0.0110 (5)	0.0083 (4)	0.0060 (4)	0.0022 (4)	0.0010 (4)
N2	0.0203 (6)	0.0139 (5)	0.0094 (4)	0.0093 (5)	0.0019 (4)	−0.0013 (4)
C1	0.0105 (5)	0.0107 (5)	0.0082 (5)	0.0046 (4)	0.0002 (4)	0.0007 (4)
C2	0.0109 (5)	0.0109 (5)	0.0106 (5)	0.0054 (4)	0.0030 (4)	0.0023 (4)
C3	0.0139 (5)	0.0121 (6)	0.0094 (5)	0.0059 (5)	0.0025 (4)	0.0006 (4)
C4	0.0121 (5)	0.0128 (6)	0.0113 (5)	0.0035 (5)	−0.0001 (4)	0.0009 (4)
C5	0.0107 (5)	0.0176 (6)	0.0130 (5)	0.0073 (5)	0.0002 (4)	0.0008 (5)
C6	0.0115 (5)	0.0143 (6)	0.0107 (5)	0.0071 (5)	0.0010 (4)	0.0005 (4)
C7	0.0118 (5)	0.0181 (6)	0.0151 (5)	0.0086 (5)	0.0035 (5)	0.0016 (5)
C8	0.0167 (6)	0.0226 (7)	0.0134 (6)	0.0050 (6)	−0.0036 (5)	−0.0036 (5)
C9	0.0186 (6)	0.0309 (8)	0.0138 (6)	0.0172 (6)	0.0002 (5)	−0.0043 (5)
C10	0.0091 (5)	0.0112 (5)	0.0094 (5)	0.0045 (4)	−0.0012 (4)	−0.0005 (4)
C11	0.0100 (5)	0.0122 (6)	0.0094 (5)	0.0044 (4)	0.0004 (4)	0.0010 (4)
C12	0.0140 (6)	0.0125 (6)	0.0132 (5)	0.0059 (5)	0.0001 (4)	−0.0003 (4)
C13	0.0143 (6)	0.0119 (6)	0.0185 (6)	0.0041 (5)	0.0009 (5)	0.0038 (5)
C14	0.0135 (6)	0.0188 (7)	0.0149 (6)	0.0052 (5)	0.0024 (5)	0.0069 (5)
C15	0.0148 (6)	0.0207 (7)	0.0116 (5)	0.0079 (5)	0.0031 (5)	0.0020 (5)
C16	0.0114 (5)	0.0137 (6)	0.0108 (5)	0.0060 (5)	0.0003 (4)	0.0006 (4)
C17	0.0195 (6)	0.0167 (6)	0.0103 (5)	0.0104 (5)	0.0025 (5)	−0.0008 (4)

Geometric parameters (Å, º)

S1—O1	1.4273 (10)	C7—H7C	0.9800
S1—O2	1.4300 (10)	C8—H8A	0.9800
S1—N1	1.7422 (11)	C8—H8B	0.9800
S1—C1	1.7646 (12)	C8—H8C	0.9800
O3—C10	1.2175 (15)	C9—H9A	0.9800
N1—N2	1.3808 (15)	C9—H9B	0.9800
N1—C10	1.4003 (17)	C9—H9C	0.9800
N2—C17	1.2911 (18)	C10—C11	1.4694 (18)
C1—C6	1.4130 (18)	C11—C12	1.3943 (19)
C1—C2	1.4142 (17)	C11—C16	1.4034 (18)
C2—C3	1.3975 (18)	C12—C13	1.3847 (19)
C2—C7	1.5066 (18)	C12—H12	0.9500
C3—C4	1.3913 (19)	C13—C14	1.400 (2)
C3—H3	0.9500	C13—H13	0.9500
C4—C5	1.3883 (18)	C14—C15	1.380 (2)

C4—C8	1.5055 (19)	C14—H14	0.9500
C5—C6	1.3917 (18)	C15—C16	1.4059 (19)
C5—H5	0.9500	C15—H15	0.9500
C6—C9	1.5125 (18)	C16—C17	1.438 (2)
C7—H7A	0.9800	C17—H17	0.9500
C7—H7B	0.9800		

O1—S1—O2	118.39 (6)	C4—C8—H8B	109.5
O1—S1—N1	106.22 (6)	H8A—C8—H8B	109.5
O2—S1—N1	104.37 (6)	C4—C8—H8C	109.5
O1—S1—C1	112.48 (6)	H8A—C8—H8C	109.5
O2—S1—C1	110.28 (6)	H8B—C8—H8C	109.5
N1—S1—C1	103.58 (6)	C6—C9—H9A	109.5
N2—N1—C10	126.97 (11)	C6—C9—H9B	109.5
N2—N1—S1	113.93 (9)	H9A—C9—H9B	109.5
C10—N1—S1	118.89 (8)	C6—C9—H9C	109.5
C17—N2—N1	116.47 (12)	H9A—C9—H9C	109.5
C6—C1—C2	121.56 (11)	H9B—C9—H9C	109.5
C6—C1—S1	117.50 (9)	O3—C10—N1	120.86 (12)
C2—C1—S1	120.94 (10)	O3—C10—C11	124.94 (12)
C3—C2—C1	117.37 (12)	N1—C10—C11	114.19 (11)
C3—C2—C7	116.62 (11)	C12—C11—C16	120.62 (12)
C1—C2—C7	126.01 (11)	C12—C11—C10	120.00 (11)
C4—C3—C2	122.42 (12)	C16—C11—C10	119.36 (12)
C4—C3—H3	118.8	C13—C12—C11	119.31 (12)
C2—C3—H3	118.8	C13—C12—H12	120.3
C5—C4—C3	118.48 (12)	C11—C12—H12	120.3
C5—C4—C8	120.39 (12)	C12—C13—C14	120.60 (13)
C3—C4—C8	121.12 (12)	C12—C13—H13	119.7
C4—C5—C6	122.33 (12)	C14—C13—H13	119.7
C4—C5—H5	118.8	C15—C14—C13	120.31 (13)
C6—C5—H5	118.8	C15—C14—H14	119.8
C5—C6—C1	117.83 (11)	C13—C14—H14	119.8
C5—C6—C9	116.57 (12)	C14—C15—C16	119.85 (13)
C1—C6—C9	125.58 (12)	C14—C15—H15	120.1
C2—C7—H7A	109.5	C16—C15—H15	120.1
C2—C7—H7B	109.5	C11—C16—C15	119.30 (13)
H7A—C7—H7B	109.5	C11—C16—C17	117.99 (12)
C2—C7—H7C	109.5	C15—C16—C17	122.69 (12)
H7A—C7—H7C	109.5	N2—C17—C16	125.01 (12)
H7B—C7—H7C	109.5	N2—C17—H17	117.5
C4—C8—H8A	109.5	C16—C17—H17	117.5

O1—S1—N1—N2	120.33 (10)	C2—C1—C6—C5	−0.2 (2)
O2—S1—N1—N2	−5.52 (11)	S1—C1—C6—C5	178.53 (10)
C1—S1—N1—N2	−120.99 (10)	C2—C1—C6—C9	−178.71 (14)
O1—S1—N1—C10	−54.70 (11)	S1—C1—C6—C9	0.02 (19)
O2—S1—N1—C10	179.45 (10)	N2—N1—C10—O3	−179.88 (12)

C1—S1—N1—C10	63.98 (11)	S1—N1—C10—O3	−5.57 (17)
C10—N1—N2—C17	−0.8 (2)	N2—N1—C10—C11	0.98 (18)
S1—N1—N2—C17	−175.38 (10)	S1—N1—C10—C11	175.29 (9)
O1—S1—C1—C6	−176.04 (10)	O3—C10—C11—C12	2.1 (2)
O2—S1—C1—C6	−41.49 (12)	N1—C10—C11—C12	−178.79 (11)
N1—S1—C1—C6	69.70 (11)	O3—C10—C11—C16	−179.23 (12)
O1—S1—C1—C2	2.71 (13)	N1—C10—C11—C16	−0.13 (17)
O2—S1—C1—C2	137.26 (11)	C16—C11—C12—C13	0.6 (2)
N1—S1—C1—C2	−111.55 (11)	C10—C11—C12—C13	179.29 (12)
C6—C1—C2—C3	0.74 (19)	C11—C12—C13—C14	−0.1 (2)
S1—C1—C2—C3	−177.95 (10)	C12—C13—C14—C15	−0.3 (2)
C6—C1—C2—C7	179.99 (13)	C13—C14—C15—C16	0.2 (2)
S1—C1—C2—C7	1.30 (19)	C12—C11—C16—C15	−0.75 (19)
C1—C2—C3—C4	−0.3 (2)	C10—C11—C16—C15	−179.40 (12)
C7—C2—C3—C4	−179.65 (12)	C12—C11—C16—C17	177.93 (12)
C2—C3—C4—C5	−0.6 (2)	C10—C11—C16—C17	−0.72 (18)
C2—C3—C4—C8	178.73 (13)	C14—C15—C16—C11	0.3 (2)
C3—C4—C5—C6	1.2 (2)	C14—C15—C16—C17	−178.29 (13)
C8—C4—C5—C6	−178.16 (13)	N1—N2—C17—C16	−0.2 (2)
C4—C5—C6—C1	−0.8 (2)	C11—C16—C17—N2	0.9 (2)
C4—C5—C6—C9	177.86 (14)	C15—C16—C17—N2	179.58 (14)

Hydrogen-bond geometry (Å, º)

D—H···*A*	*D*—H	H···*A*	*D*···*A*	*D*—H···*A*
C12—H12···O2^{i}	0.95	2.49	3.3395 (18)	149

Symmetry code: (i) *x*, *y*−1, *z*.